THERMALLY-INDUCED BOWING OF CANDU FUEL ELEMENTS

H.C. Suk, K.S. Sim, J.H. Park and G.S. Park
Korea Atomic Energy Research Institute
P.O.Box 105, Yusung, Taejon City, 305-600, Republic of Korea

ABSTRACT

Considering only the thermally-induced bending moments which are generated both within the sheath and between the fuel and sheath by a asymmetric temperature distribution with respect to the axis of an element, a generalized and explicit analytical formula for the thermally-induced bending is developed in this paper, based on the cases of 1) the bending of an empty tube treated by neglecting of the fuel/sheath mechanical interaction and 2) the fuel/sheath interaction due to the pellet and sheath temperature variations. In each the cases, the temperature asymmetries in sheath are modelled to be caused by the combined effects of (i) non-uniform coolant temperature due to imperfect coolant mixing, (ii) variable sheath/coolant heat transfer coefficient, (iii) asymmetric heat generation due to neutron flux gradients across an element and so as to inclusively cover the uniform temperature distributions within the fuel and sheath with respect to the axial centerline.

Investigating the relative importances of the various parameters affecting fuel element bowing, the element bowing is found to be greatly affected with the variations of element length, sheath diameter, pellet/sheath mechanical interaction and neutron flux depression factors, pellet thermal expansion coefficient, pellet/sheath heat transfer coefficient in comparison with those of other parameters such as sheath thickness, film heat transfer coefficient, sheath thermal expansion coefficient, and sheath and pellet thermal conductivities.

Also, the element bowing of the standard 37-element bundle and CANFLEX 43-element bundle for the use in CANDU-6 reactors was analyzed with the formula, which could help to demonstrate the integrity of the fuel. All the required input data for the analyses were generated in terms of the reactor operation conditions on the reactor physics, thermalhydraulics and fuel performance by using various CANDU computer codes. The analysis results indicate that the CANFLEX 43-element bundle shows more desirable element bowing behaviours than the standard 37-element bundle.

1. INTRODUCTION

Assessments of bowing of nuclear fuel elements can help demonstrate the integrity of fuel and of surrounding components during irradiation, as a function of operating conditions such as channel power. The bowing is defined as the lateral deflection of the element from the axial centerline during irradiation, and the magnitude of the bow is the maximum defection between points of restraint. Bowed fuel elements could reduce subchannel flow area resulting in poor heat transfer due to local coolant starvation and these elements may consequently defect as a result of local overheating. Another phenomenon which is attributed partially to bowing and partially to irradiation induced swelling is the 'sticking' of bundles in a fuel channel. If 'sticking' occurs, more force is required during bundle shifting and removal during the refuelling process.

The element bowing is attributed to actions of both the thermally induced bending moments and the bending moments due to hydraulic drag and mechanical loads during the refuelling process, and is restrained by the appendages, end plates and neighboring elements of the bundle. The thermally-induced bending moments are generated both within the sheath and between the fuel and sheath by an asymmetric temperature distribution with respect to the axis of an element. One side of the element becomes hotter than the other and the element bows in the direction of the hotter side to accommodate the differential axial strain. The temperature variations around the fuel and sheath set up the bend moments.

Based on these phenomena, Veeder and Schankula[1] developed analytically a time-independent model of the thermally-induced bowing theory of fuel elements which are constituents of fuel bundles similar in size and shape to those used in CANDU (Canada deuterium uranium) power reactors [2]. Fig. 1 shows a typical CANDU fuel bundle. Their analysis was basically hypothesized that bowing of pelletized fuel elements of the type under consideration is primarily a thermally induced phenomenon. Based on the Veeder and Schankula model, Tayal [3] developed the BOW code to calculate the bowing of CANDU fuel elements due to gradients of temperature and due to hydraulic forces. It is noted that the variations of the coolant temperature and film heat transfer coefficient are neglected in their final formula for the element bowing, and that their formula of the sheath temperature variations and so deflections are not adequately derived. To cope with these neglects and improper derivation of the bowing formula, an improvement of the bowing analysis model has been done through re-assessment of Veeder and Schankula model and so resulted in a generalized formula for the thermally-induced bowing calculation [4].

This paper presents the thermally-induced bowing modeling and time-independent, generalized and explicit analytical formula for the calculations of the temperature variations and hence the bending moments by considering the peripheral temperature gradients caused by them. It also outlines the method of all the required input data generations for the analyses in terms of CANDU-6 reactor operating conditions on the reactor physics, thermalhydraulics and fuel performance by using various CANDU computer codes.

Also this paper describes a parametric study on the generalized bowing formula to investigate the influence of the variation or change of an element geometric, material or operation parameters such as one of element length, sheath inside diameter, coolant temperature variation factor, a factor of mechanical interaction between fuel pellet and sheath, neutron flux depression factor, pellet thermal expansion coefficient, pellet/sheath heat transfer coefficient, sheath thickness, film heat transfer coefficient, sheath thermal expansion coefficient, and sheath and pellet thermal conductivities on the element bowing.

Finally, this paper shows the thermally-induced element bowing behaviours of the standard 37-element bundle and CANFLEX (CANdu FLEXible fuelling) 43-element bundle in CANDU-6 reactor by analyzing them with the formula, which could help to demonstrate the integrity of the fuel. It is also interested in the comparisons of the element bowing behaviours of CANFLEX 43-element bundle with that of the standard 37-element bundle. CANFLEX is a 43-element, CANDU advanced fuel bundle under joint development by KAERI (Korea Atomic Energy Research Institute) and AECL (Atomic Energy of Canada Limited) since February 1991 [5]. The major feature of the CANFLEX fuel bundle is an increase in the number of fuel elements, from 37, 13.1 mm diameter elements in the standard CANDU-6 fuel bundle, to 43 elements of two different diameters. The 11.5 mm diameter elements in the outer two rings of the CANFLEX fuel bundle allow the peak element ratings in the bundle to be reduced by about 20 % in comparison to the standard 37-element bundle. The 13.5 mm diameter elements in the inner two rings of the CANFLEX fuel bundle compensate for the fuel volume lost due to the smaller-diameter outer elements. Another important feature is the use of CHF-enhancing features on all elements in the CANFLEX fuel bundle. These will provide larger operating margins in existing CANDU reactors, thus permitting more flexibility in the use of fuel cycles with the CANDU-reactor on-power fuelling system.

Notation used in this paper are listed at the last page of this paper.

2. MODELING AND FORMULATING OF THE BOWING

2.1 Basic Hypotheses and General Solutions of Heat Conduction Equations

The model for the thermally-induced bowing of CANDU fuel elements presented in this paper is based on the three basic hypotheses from which the in-reactor bowing of pelletized fuel elements is considered to cause bending moments both within the sheath and between the fuel and sheath due to the peripheral temperature gradients by:

(1) non-uniform coolant temperature due to imperfect coolant mixing,
(2) variable heat transfer coefficient between fuel and coolant, and
(3) asymmetric heat generation due to neutron flux gradients across an element,

These inclusively cover the uniform temperature distributions within the fuel and sheath with respect to the axial centerline.

The generalized and explicit analytical formulas for the thermally-induced bending can be derived with consideration of 1) bending of an empty tube treated by neglecting of the fuel/sheath mechanical interaction and 2) interaction between fuel pellet and sheath due to the pellet and sheath temperature variations.

The coordinate system used in the present model is shown in Fig. 2. The angle θ is measured in the clockwise direction from the vector CO. From the geometry of the bundle we make the plausible assumption that the temperature distributions within the fuel and sheath are symmetrical about the vector CO. It is also assumed that the neutron flux distribution through the bundle can approximately described by a modified Bessel function $I_0(\kappa R)$, where κ is the inverse diffusion length for thermal neutrons in the homogenized fuel channel (fuel, coolant and sheath) and R is the displacement between the center of bundle and center of element under consideration :

$$I_0(\kappa R) = I_0(\kappa R_i)\, I_0(\kappa r) + 2\sum_{m=1}^{\infty}(-1)^m\, I_m(\kappa R_i)\, I_m(\kappa r)\cos m\theta \qquad (2.1\text{-}1)$$

If the fuel thermal conductivity, λ, is a constant value, the heat conduction equation in the fuel with asymmetric heat generation in the cylindrical coordinates becomes

$$\frac{1}{r}\frac{\partial}{\partial r}\left(r\frac{\partial T}{\partial r}\right)+\frac{1}{r^2}\frac{\partial^2 T}{\partial \theta^2} = -\frac{q_o'''}{\lambda}\, I_0(kR) \qquad (2.1\text{-}2)$$

where q_o''' (r, R=0) is the power per unit volume at the center of flux symmetry.

The heat conduction equation for the region of sheath in which the heat generation is negligible is given by

$$\frac{1}{r}\frac{\partial}{\partial r}\left(r\frac{\partial T}{\partial r}\right)+\frac{1}{r^2}\frac{\partial^2 T}{\partial \theta^2} = 0 \qquad (2.1\text{-}3)$$

A general solution to the heat conduction equation of Eq. (2.1-2) can be expressed as

$$T(r,\ \theta) = A_o + A\, I_o(\kappa R) + \sum_{m=1}^{\infty} A_m\, r^m \cos m\theta \qquad (2.1\text{-}4)$$

where A_o represents the centerline temperature, and A is given by

$$A = \frac{-q'}{2\pi\,\lambda\,\kappa a I_o(\kappa R_i)\, I_1(\kappa a)} \qquad (2.1\text{-}5)$$

A general solution to Eq.(2.1-3) can be obtained for the region of sheath:

$$T_s(r,\ \theta) = B_o + B\ln r + \sum_{m=1}^{\infty}\left(B_m\, r^m + \frac{C_m}{r^m}\right)\cos m\theta \qquad (2.1\text{-}6)$$

2.2 Boundary Conditions of the Heat Conduction Equations

The coefficients in Eqs. (2.2.1-4) and (2.2.1-6) are determined the following boundary conditions for the elements with asymmetric or symmetric heat generation in coolant with non-uniform temperatures due to imperfect mixing and non-uniform film heat transfer between sheath and coolant and are by equating terms in cos mθ:

(a) Coolant temperature variation at r = b:

$$T_c = \overline{T}_c\,(1+\beta \cos\theta) \qquad (2.2\text{-}1)$$

where $$\beta = \frac{T_c(\max) - T_c(\min)}{T_c(\max) + T_c(\min)} \qquad (2.2\text{-}2)$$

(b) Continuity of heat flux at r = a:

$$\lambda \frac{\partial T}{\partial r}\bigg|_{r=a} = \lambda_s \frac{\partial T_s}{\partial r}\bigg|_{r=a} \quad \text{and} \quad -\lambda \frac{\partial T}{\partial r}\bigg|_{r=a} = h_{fs}\,(T - T_s)\big|_{r=a} \qquad (2.2\text{-}3)$$

(c) Continuity of heat flux at r = b:

$$-\lambda_s \frac{\partial T_s}{\partial r}\bigg|_{r=b} = h_{sc}\,(T_s - T_c)\big|_{r=b} \qquad (2.2\text{-}4)$$

where $$h_{sc} = \overline{h}_{sc}\,(1+\gamma \cos\theta) \qquad (2.2\text{-}5)$$

$$\gamma = \frac{h_{sc}(\max) - h_{sc}(\min)}{h_{sc}(\max) + h_{sc}(\min)} \qquad (2.2\text{-}6)$$

2.3 Formulation of Bowing

2.3.1 Bending of an empty tube

The fuel sheath can be treated as an empty tube, if the mechanical interaction between the sheath and fuel pellets is neglected. The empty tube bending moment due to temperature variation within the sheath can be found by using the following formula [6]:

$$M_s = \alpha_s E_s \int_a^b \int_0^{2\pi} T_s \cos\theta \; r^2 \, dr\, d\theta \qquad (2.3\text{-}1)$$

and substituting Eq.(2.1-6) with m = 1 into Eq.(2.3-1) this becomes

$$M_s \approx \frac{\pi \alpha_s E_s}{4}\left[B_1 (b^4 - a^4) + 2 C_1 (b^2 - a^2)\right] \qquad (2.3\text{-}2)$$

In a CANDU bundle, the end caps are welded to the ends of the sheaths to seal the elements. End plates are welded to the end caps to hold the elements in the bundle assembly. So the sheaths can be assumed in hinged end conditions. Therefore, the deflection δ of the sheath at the mid-span due to the bending moment is given by

$$\delta \approx \frac{M_s l^2}{8 E_s I_s} \approx \frac{l^2 \alpha_s}{8\,b}\left[B_1\, b + \frac{C_1}{b}\right] \qquad (2.3\text{-}3)$$

in which $I_s = \pi (b^4 - a^4)/4$ is used for the moment of inertia, I_s, of a hollow tube of thickness $t = b - a$ and then $t/b \approx 0$ is counted for the thinned walled tube. Veeder and Schankula [1] noted that the hinged end condition was found experimentally to be a good approximation for elements in the type of fuel bundles under investigation at AECL.

Since the maximum surface temperature of sheath is given by setting m = 1 and $\theta = 0$ or 2π in Eq.(2.1-6), and the minimum surface temperature of sheath is given by setting m = 1 and $\theta = \pi$ in Eq.(2.1-6), the bracketed term in Eq.(2.3-3) is reduced to be approximately equal to half of the difference between the maximum ($T_{s,max}$) and minimum ($T_{s,min}$) surface temperatures of sheath:

$$B_1 \bar{b} + \frac{C_1}{b} \approx \frac{T_{s,max} - T_{s,min}}{2} \equiv \frac{\Delta T_s}{2} \qquad (2.3\text{-}4)$$

where B_1 and B_2 are determined by applying the boundary conditions in Section 2.2.

Cooperating Eqs. (2.1-4) and (2.1-6) with the boundary conditions in Section 2.2 where m = 1 shall be provided, the half of the difference between the maximum and minimum surface sheath temperatures is obtained :

$$\left(B_1 b + \frac{C_1}{b}\right) = \left\{aK_1\left[\bar{h}_{sc}(1-\gamma^2)\beta\ \bar{T}_c - \gamma\ \bar{w}\right] - 2b\bar{w}D\right\} / K_2 \qquad (2.3\text{-}5)$$

This equation gives the difference ΔT_{SE} between the maximum and minimum surface temperatures of sheath according to Eq. Eq.(2.3-4), and the deflection δ_{SE} of the empty tube according to Eq. (2.3-3):

$$\Delta T_{SE} \approx 2\left\{aK_1\left(\bar{h}_{sc}(1-\gamma^2)\beta\ \bar{T}_c - \gamma\ \bar{w}\right) - 2b\bar{w}D\right\} / K_2 \qquad (2.3\text{-}6)$$

$$\delta_{SE} \approx \frac{l^2\ \alpha_s}{8\ b\ K_2}\left\{aK_1\left(\bar{h}_{sc}(1-\gamma^2)\beta\ \bar{T}_c - \gamma\ \bar{w}\right) - 2b\bar{w}D\right\} \qquad (2.3\text{-}7)$$

where

$$K_1 = 1 + \frac{\lambda}{a\ h_{fs}} + \frac{\lambda\ t}{a\ \lambda_s} \qquad (2.3\text{-}8)$$

$$K_2 = \lambda + a\ \bar{h}_{sc}(1-\gamma^2)\left(1 + \frac{\lambda}{a\ h_{fs}} + \frac{\lambda\ t}{a\ \lambda_s}\right) \qquad (2.3\text{-}9)$$

$$\bar{w} = \frac{q'}{2\pi\ b} \qquad (2.3\text{-}10)$$

$$D = \frac{I_1(\kappa R_i)\ I_2(\kappa a)}{I_0(\kappa R_i)\ I_1(\kappa a)} \qquad (2.3\text{-}11)$$

in which $\bar{w}$ is the average heat flux of the element and D is a factor determined by the flux depression through the fuel bundle.

2.3.2 Bending due to interaction between pellet stack and sheath

The fuel pellet stack is a column of ceramic fuel pellets within the sheath. Each of the pellets cracks into many smaller pieces during irradiation. The fuel stack is therefore incapable of sustaining an applied bending moment. If, however, the sheath is collapsed into the pellets or the fuel grips the sheath, it can induce a bending moment in the sheath, because the thermal expansion of the sheath at the interface is smaller than that of the pellet. Assuming that the strength of the sheath is insufficient to resist the thermal expansion of the fuel, the component of strain due to the elastic stress in the sheath can be ignored. Based on this assumption, at the point (a, θ), the difference in longitudinal thermal strain between the fuel and sheath is given by

$$\Delta S(a, \theta) = \alpha T(a, \theta) - \alpha_s T_s(a, \theta) \tag{2.3-12}$$

and

$$T(a, \theta) - T_s(a, \theta) = -\frac{\lambda}{h_{fs}} \frac{\partial T}{\partial r}\bigg|_{r=a} \tag{2.3-13}$$

which is provided by Eq.(2.2-3). If there is no slip between fuel stack and sheath, the sheath will be strained in the axial direction by an amount equal to the differential thermal strain, and if there is some slip between them, the mechanical strain will be less than the differential thermal strain. Therefore, a relationship between the differential thermal strain and the induced mechanical strain can be expressed by

$$\Delta\varepsilon\ (a, \theta) = G\,\Delta S(a, \theta) \tag{2.3-14}$$

where G is a factor between 0 and 1. Veeder and Schankula[1] indicated that G is about 0.5 according to the calculations for a free standing sheath having a diametral clearance of 0.08 mm with the CANDU fuel modeling code ELESTRES[7] and so the collapsibility of the sheath implies a value of G greater than 0.5. Substituting Eqs. (2.3-12) and (2.3-13) into Eq. (2.3-14) gives

$$\Delta\varepsilon\ (a, \theta) = G\left\{\left[(\alpha - \alpha_s)T(a, \theta)\right] - \frac{\lambda\,\alpha_s}{h_{fs}} \frac{\partial T}{\partial r}\bigg|_{r=a}\right\} \tag{2.3-15}$$

Also, cooperating Eqs. (2.1-4) and (2.1-6) with the boundary conditions at r = a and m = 1, the strain relationship of Eq.(2.3-15) is given by

$$\Delta\varepsilon\ (a, \theta) \approx G\left\{K_3\bar{T}_c(1+\beta\cos\theta) - Z + K_4\left[\left(\frac{\lambda\gamma\bar{w} - 2\bar{h}_{sc}(1-\gamma^2)b\bar{w}D}{K_2}\right)\right.\right.$$
$$\left.\left. - \beta\,\bar{T}_c\left(\frac{\lambda\,\bar{h}_{sc}(1-\gamma^2)}{K_2}\right)\right]\cos\theta\right\} \tag{2.3-16}$$

where

$$K_3 = \alpha - \alpha_s \tag{2.3-17}$$

$$K_4 = (\alpha - \alpha_s)\left(\frac{1}{h_{fs}} + \frac{t}{\lambda_s} + \frac{1}{\bar{h}_{sc}}\right) + \frac{\alpha_s}{h_{fs}} \tag{2.3-18}$$

$$Z = A\lambda K_4 \kappa I_0(\kappa R_i) I_1(\kappa a).$$

Cooperating Eq.(2.3-16) with Eq.(2.3-1), the induced bending moment in the sheath is given by

$$M_s = E_s\,a^2\,t \int_0^{2\pi} \Delta\varepsilon\ (a, \theta)\cos\theta\,d\theta \tag{2.3-19}$$

The deflection δ_{SI} due to the bending moment at the mid-span is given by assuming the hinged end conditions and by noting that terms in the integration of Eq. (2.3-19) which are independent of θ vanish when integrated between the limits, as do all terms in cos θ

$$\delta_{SI} \approx \frac{M_s\,l^2}{8\,E_s\,I_s} \approx \frac{G l^2}{8\,a}\left\{\beta\,\bar{T}_c\left(K_3 - \frac{K_4\lambda\,\bar{h}_{sc}(1-\gamma^2)}{K_2}\right)\right.$$
$$\left. + \frac{K_4\bar{w}\left(\lambda\gamma - 2\bar{h}_{sc}(1-\gamma^2)bD\right)}{K_2}\right\} \tag{2.3-20}$$

$$= \frac{l^2\alpha_s}{16\,b}\left\{\frac{2Gb}{a\alpha_s}\left(\beta\,\overline{T}_c\left(K_3 - \frac{K_4\,\lambda\,\overline{h}_{sc}(1-\gamma^2)}{K_2}\right)\right) + \frac{K_4\overline{w}(\lambda\,\gamma - 2\overline{h}_{sc}(1-\gamma^2)bD)}{K_2}\right\} \quad (2.3\text{-}21)$$

in which the moment of inertia, $I_s = \pi\ a^3 t$ is used for the thin walled tubing.

Noting Eqs.(2.3-6) and (2.3-7), the term in the brackets of the Eq.(2.3-21) may be arbitrarily regarded as being equivalent to a temperature difference ΔT_{SI}, across the sheath which would produce a deflection equal to that caused by interaction between fuel pellet and sheath. Thus,

$$\Delta T_{SI} \approx \frac{2Gb}{a\alpha_s}\left\{\beta\,\overline{T}_c\left(K_3 - \frac{K_4\lambda\,\overline{h}_{sc}(1-\gamma^2)}{K_2}\right) + \frac{K_4\overline{w}(\lambda\,\gamma - 2\overline{h}_{sc}(1-\gamma^2)bD)}{K_2}\right\} \quad (2.3\text{-}22)$$

2.3.3 Bowing combined effects of the empty tube bending and pellet/sheath interactions

In Section 2.3.2, the element bowing at the point (a, θ) is due to the difference in longitudinal thermal strain between the fuel and sheath for the interaction between pellet stack and sheath. This element bowing does not include the effect of the bending moment due to temperature variation within the sheath as treated in Section. 2.3.1. So the element bowing combined effects of the empty tube bending and pellet/sheath interaction shall be formulated by adding Eq.(2.3-6) with Eq.(2.3-22) for ΔT_{SC} and adding Eq.(2.3-7) with Eq.(2.3-20) for δ_{SC} :

$$\Delta T_{SC} \approx \frac{2\left\{aK_1\left(\overline{h}_{sc}(1-\gamma^2)\beta\,\overline{T}_c - \gamma\overline{w}\right) - 2b\overline{w}D\right\}}{K_2} + \frac{2Gb}{a\alpha_s}\left\{\beta\,\overline{T}_c\left(K_3 - \frac{K_4\lambda\,\overline{h}_{sc}(1-\gamma^2)}{K_2}\right) + \frac{K_4\overline{w}(\lambda\gamma - 2\overline{h}_{sc}(1-\gamma^2)bD)}{K_2}\right\} \quad (2.3\text{-}23)$$

$$\delta_{SC} \approx \frac{l^2\,\alpha_s\left\{aK_1\left(\overline{h}_{sc}(1-\gamma^2)\beta\,\overline{T}_c - \gamma\overline{w}\right) - 2b\overline{w}\,D\right\}}{8\,b\,K_2} + \frac{Gl^2}{8\,a}\left\{\beta\,\overline{T}_c\left(K_3 - \frac{K_4\lambda\,\overline{h}_{sc}(1-\gamma^2)}{K_2}\right) + \frac{K_4\overline{w}(\lambda\gamma - 2\overline{h}_{sc}(1-\gamma^2)bD)}{K_2}\right\} \quad (2.3\text{-}24)$$

3. METHOD OF THE BOW FORMULA'S INPUT DATA GENERATION IN TERMS OF CANDU-6 OPERATING CONDITIONS

In order to investigate the thermally induced element bowing behaviours of the standard 37-element and CANFLEX 43-element bundles in CANDU-6 reactor as well as to illustrate the relative importances of the various parameters affecting fuel element bowing, the numerical values of the parameters associated with the reactor physics, thermal hydraulic, and element and material performances are generated by simulating the CANDU-6 full power operation with the standard 37-element and CANFLEX 43-element natural UO_2 fuel bundles :

1) The bundle and element dimensions are taken from the nominal design values.

2) The channel and fuel bundle power histories for the given bundle and element geometries are obtained from the RFSP [8] refuelling simulation of the CANDU-6 full power reactor operation from an equilibrium core condition to 600 full power days (FPD), based on the reference eight-bundle refuelling. With the WIMS-AECL [9], the bundle's ring power ratio, element power (q') and neutron flux depression factor (D) associated with Eq.(2.3-24) are estimated from the bundle power histories. For given CANDU fuel element and bundle geometries, the element bowing is strongly dependent on the operating power history and coolant conditions as discussed below. Therefore, the representative bundles for the present element bow assessment are selected from those loaded in the highest power channel (N-6) in CANDU-6. According this simulation, one batch of 8 fuel bundles is refuelled and placed in, so to say, P-1 to P-8 positions from the upstream of the N-6 channel at 100 FPDs. The 4 fuel bundles in the channel upstream positions P-1 to P-4 are moved to the positions, so to say, P-9 to P-12 in the channel downstream by refuelling at 280 FFDs, and then are discharged at 490 FPD. The remaining 4 fuel bundles in the channel upstream positions P-6 to P-8 are discharged at 280 FFDs. Among these bundles, the two bundles in the positions of P-4 and P-6 are selected as the representative bundles for the present calculations, because (i) the fuel bundle in the P-6 position is irradiated with the continuous highest bundle power and (ii) the outer and intermediate rings of the end plate of the last downstream bundle B-4 in the P-12 position are contacted with both the shield plug and ram adaptor during the in-reactor service and the refuelling after 280 FPDs.

3) With NUCIRC single channel analysis code [10], the channel flow and heat flux of the given bundle and element geometries are calculated for the given channel power, head-to-head pressure drop and pressure loss coefficients of bundles. The subchannel flow characteristics are analyzed with use of COBRA-IIIc code[11], providing the results of single channel analysis as the boundary conditions. The subchannel characteristics were analyzed by taking 1/12 and 1/14 symmetric geometries, respectively, for the 37- and 43-element bundles as shown in Fig. 3. The subchannel flow characteristics are coolant temperature, film heat transfer coefficients which are associated with Eq. (2.3-24).

4) As the parameters employed in Eq. (2.3-24), the thermal expansion coefficients and conductivities of fuel and sheath, the film heat transfer coefficient and the mechanical interaction factor G are estimated with ELESTRES[7] and the MATPRO's formulas[12], providing the element dimensions and power histories and the coolant characteristics. That is, providing these material average temperatures from the calculations with ELESTRES, the thermal expansion coefficients are calculated by using the MATPRO's formulas[12]. The G is conservatively estimated from the relationship, $G = 1 - (G_{operation} / G_{fresh\ element})$, where $G_{operation}$ is the diametral gap in the operation and so then calculated by ELESTRES and $G_{fresh\ element}$ is the diametral gap measured or calculated in the fresh element condition.

For example, the numerical values of the pertinent parameters are given in Table 1 by taking the data generation method mentioned above. This table is only made for a parametric study on the generalized bowing formula to illustrate the relative importances of the various parameters affecting fuel element bowing in the following section. The parameter values in Table 1 are taken to explain bowing in CANDU type fuel elements without having to invoke other mechanisms such as compressive axial loads.

4. RESULTS AND DISCUSSIONS

During CANDU-6 fuel bundle irradiations, the radial distributions of neutron flux and subchannel coolant temperatures through the fuel bundle are considered to be symmetrical about the bundle axis centerline. So, the neutron flux distribution in the center element and coolant temperature distribution around the element periphery will be symmetrical about the element axis centerline. But, the neutron flux distributions in the elements in the outer, intermediate and inner rings of the bundle and coolant temperature distributions around the their periphery will be asymmetrical about the element axis centerline. In this paper, a generalized and explicit analytical formula for the thermally-induced bowing of CANDU fuel elements is developed as Eq.(2.3-24) in consideration of all the elements with symmetric or asymmetric neutron and/or coolant temperature distribution(s), It is noted that Eqs.(2.3-6), (2.3-16) and (2.3.-22) are comparable with Veeder and Schankula's equations (11), (16) and (20) in Reference 1, respectively, where Veeder and Schankula's equations (11) and (20) do not properly_treat the effects of the coolant temperature and film heat_transfer coefficient variations, and Veeder and Schankula's equations (11) and (16) can not be derivable.

4.1 Relative Importances of the Parameters Affecting the Fuel Element Bowing,

To illustrate the relative importances of the various parameters affecting fuel element bowing, the element deflection, δ_{SC} of Eq. (2.3-24), was calculated for an element in the outer ring of the 37-element natural UO_2 fuel bundle.

The sensitivities of the parameters employed in Eq. (2.3-24) are shown in Figs. 4 and 5 for the asymmetric and symmetric heat generating fuel elements, respectively, where the variation was made for each one of β, γ, G, q', D, h_{fs}, α_s, α, λ_s, λ and t in the equation for all the other fixed parameters. The horizontal axis in Figs. 4 and 5 represents a normalized scale, N, for the variations of the parameters where N = 51.6 corresponds to each the values of the parameters valued in Table 1. The vertical axis in Figs. 4 and 5 as well as in Figs. 6 and 7 represents the deflections of the elements at the mid-span , and its negative or positive value refers to the element deflection in the direction of the pressure tube wall or the bundle center side.

(1) The term and factor G of the pellet/sheath interaction

For the instance of the fuel element characterized in Table 1, the bowing (0.02 mm) due to the empty tube term as the first term in the right hand side of Eq.(2.3-24) is in the direction of the bundle center because the temperature of sheath outer-surface faced to fuel bundle center is hotter than that faced to the pressure tube wall , due to the hotter coolant temperature in the bundle center side. While, the bowing (0.35 mm) due to the pellet/sheath interaction term as the second term also in the right hand side is the direction of the pressure tube wall because the temperature of sheath inner surface faced to the pressure tube wall is hotter than that faced to the fuel bundle center, due to the small neutron flux gradients in the pressure tube wall side. The net bending (0.33 mm) towards the pressure tube wall. The mechanical interaction between the pellet stack and the sheath has, in this instance, about 18 times greater effect on the element bowing than the empty tube as in the non-interaction between the pellet and the sheath. Since the pellet/sheath interaction predominates, the element bowing will be a tendency to bow out towards the wall of the pressure tube.

Changing with G = 0.0 to + 1.0 only in Eq.(2.3-24), the bows of the elements with the asymmetric and symmetric heat increases significantly, as expected, as a linear function of G (see Figs. 4 and 5), where their deflections are in the opposite directions between each other. So, if the element has a pellet/sheath mechanical interaction, the bending will increases almost in proportion to the mechanical interaction factor G.

(2) The element length and sheath inner radius and thickness

Comparing between the pellet/sheath interaction and non-interaction terms mentioned above, the net bending is realized to increases almost in direct proportion to the square of the element length l, and almost in inverse proportion to the inner radius a of sheath.

With the increase of sheath thickness t only in Eq.(2.3-24), the bowing of the element with the asymmetric heat is slowly and linearly raised in the direction of the pressure tube wall (see Fig. 4) because of the hotter temperature of sheath inner surface in the pressure tube wall side, and that with the symmetric heat, however, was slowly and linearly reduced in the direction of the bundle center (see Fig. 5) because of the hotter coolant temperature in the bundle center side.

(3) The asymmetric or symmetric heat generation in fuel, the element linear power q' and the neutron depression factor D

The fuel element with an asymmetric heat ($D \neq 0$) will bow out towards the wall of the pressure tube (see Fig. 4), because the neutron flux gradient across the element is more affected in the bowing. However, the element with a symmetric heat ($D= 0$) will bow out towards the bundle center (see Fig. 5) because of the hotter coolant temperature in the bundle center side.

With the increase of q' value only in Eq.(2.3-24), the bowing of the element with the asymmetric heat increases significantly and linearly (see Fig, 4), and however, that with the symmetric heat decreases slowly and linearly (see Fig. 5).

With the increase of neutron flux depression factor D value only in Eq.(2.3-24), the bowing of the element with the asymmetric heat increases stiffly and linearly (see Fig. 4). If there is no neutron flux depression ($D = 0$) in the element, however, the element will be in a constant deflection in the direction of the bundle center side as expected.

(4) β and γ factors for the coolant temperature and film heat transfer variations

With the increase of β value only in Eq.(2.3-24), the bowing of the element with the asymmetric or symmetric heat decreases stiffly and linearly (see Figs. 4 and 5).

With the increase of γ value only in Eq.(2.3-24), the bowing of the element with the asymmetric heat increases slowly and linearly (see Fig. 4), and however, that with the symmetric heat decreases slowly and linearly (see Fig. 5).

So it can be noted that the effect of the γ variation on the element bowing is not greater than that of β variation, and also that the variation of β value will results to significantly different results of the element deflections.

(5) The coefficients (h_{fs}, α_s, α) and the thermal conductivities (λ_s, λ)

With the increase of h_{fs} value only in Eq.(2.3-24), the bowing of the element with the asymmetric heat decreases exponentially with a rather stiff slope for the range of h_{fs} = 0.001 to about 30 kW/m^{2}K and with a rather flattened slope for the range of h_{fs}= about 30 to 90 kW/m^{2}K (see Fig. 4).

As shown in Figs. 4 and 5, the bowing of the element with the asymmetric or symmetric heat is slowly and linearly reduced with the increase of α_s value only in Eq.(2.3-24), and increases stiffly and linearly with the increase of α value only in Eq.(2.3-24)

With the increase of λ_s value only in Eq.(2.3-24), the bowing of the element with the asymmetric heat decreases stiffly and exponentially (see Fig. 4), but that with the symmetric heat decreases slowly and exponentially (see Fig. 5).

With the increase of λ value only in Eq.(2.3-24), the bowing of the element with the asymmetric or symmetric heat decreases slowly and linearly (see Figs. 4 and 5).

4.2 Element Bowing of the 37- and 43-Element Bundles in CANDU-6

The two bundles in the CANDU-6 highest power channel, N-6 were selected as the representative bundles for the present bowing analyses. One bundle B-4, which is either the 37- or 43-element bundle, so to say, at the P-4 position, has been operated with the high power of around 700 kW in the operation of the 100 to 280 FPDs and with the low power of around 150 kW at the P-12 downstream position in the operation of the 280 FFDs to the discharge at 490 FPDs. The other bundle B-6, which is either the 37- or 43 bundle at the P-6 position, has been operated with the continuous highest power of around 800 kW in the fuel string in the operation of the 100 FPDs to the discharge at 280 FPs.

Figs. 6 and 7 show the thermally-induced element bows of the 37- and 43-element bundles, which are estimated by Eq.(2.3-24) with the input described earlier.

(1) The Elements of the Fuel Bundles with a Stepwise Power History

The thermally-induced bows of the intermediate element (E3) and outer elements (E4 and E5) of the B-4 37-element bundle at the P-4 position in the high power operation until 280 FPDs were in direction of the pressure tube wall (see Fig. 6 (A)), while the those at the P-12 position in the low bundle power operation after the refuelling at 280 FPDs was switched to the direction of the bundle center. The bowing of inner element (E2) of the B-4 bundle in the high power operation was in the direction of the bundle center, and that in the low power operation was in the direction of the pressure tube wall until about 360 FPDs operation and then was in the direction of the bundle center after the operation at about 360 FPDs. The bowing of outer elements is larger than that of other elements, because the outer elements have high power than the other elements.

The thermally-induced bows of the intermediate element(E3) and outer elements (E4 and E5) of the 43-element bundles at the P-4 position in the high power operation until 280 FPDs were in the direction of the pressure tube wall (see Fig. 6 (B)), while those at the P-12 position in the low bundle power operation after the refuelling at 280 FPDs was switched in the direction of the bundle center. The bowing of inner element (E2) for all the high and low bundle power operations was in the direction of the bundle center, even if a transient bowing appeared in the power change during the refuelling at 280 FPDs. The inner element bowing is larger for the high bundle power operation until 280 FPDs and the outer element bowing is larger for the low bundle power operation after 280 FPDs, since the inner elements have high power in the early burnup stage in comparison with the outer elements.

As shown in Figs. 6 (A) and (B) of the element bows of the bundle at the positions of P-4 and P-12, the maximum thermally-induced element bowing of the 37-element bundle occurred in the outer element at around 280 FPDs just before the refuelling and was in the direction of the pressure tube wall side, while that of the 43-element bundle at the same positions of B-4 and B-12 occurred in the inner element at around 140 FPDs as a rather early burnup stage and was also in the direction of the pressure tube wall. The maximum thermally-induced element bowing of 37-element bundle was 0.15 mm, which was about 30 % larger than that of the 43-element bundle.

(2) The Elements of the Fuel Bundles with a Continuous High Power History

The thermally-induced bowing of the intermediate element (E3) and outer elements (E4 and E5) of the 37-element bundle at the P-6 position in the operation of the continuous high power from the loading at 100 FPDs to the discharge at 290 FPDs was in the direction of the pressure tube wall (see Fig. 7 (A)). The intermediate element bow gradually and slightly decreased with the increase of the burnp, while the outer element bows gradually increased with the increase of the burnup. The thermally-induced bow of the inner elements during the in-reactor service was almost constant in the direction of the bundle center.

The thermally-induced bowing of all the inner, intermediate and outer elements of the

B-6 43-element bundle at the P-6 position in the continuous high bundle power operation from the loading at 100 FPDs to the discharge at 290 FPDs was in the direction of the pressure tube wall (see Fig. 7(B)). All the element bows gradually decreased with the increase of the burnup.

As shown in Figs. 7 (A) and (B), the maximum thermally-induced bowing of the 37-element bundle at the P-6 position occurred in the outer element at around 280 FPDs just before the refuelling and was in the direction of the pressure tube wall. While, that of the 43-element bundle at the same position of P-6 occurred in the inner element at around 140 FPDs as a rather early burnup stage and was also in the direction of the pressure tube wall. The maximum thermally-induced element bow of 37-element bundle was 0.22 mm which was about 2 times larger than that of the 43-element bundle. It is noted that the outer element bowing of the 37-element bundle is going to be more unstable since it is increased with the increase of the burnup, while all the element bows of the 43-element bundle are going to be more stable since it is gradually disappeared when the burnup is increased.

5. SUMMARY AND CONCLUSIONS

(1) Eq. (2.3-24) is explicitly and analytically generalized for the predictions of the thermally induced element bowing. The fuel/sheath mechanical interaction factor G in the equation is an empirical factor and so is required to find appropriate value by experiments or computer simulation with existing irradiation data in a long term It is noted that Eqs.(2.3-6), (2.3-16) and (2.3.-22) are comparable with Veeder and Schankula's Eqs. (11), (16) and (20) in Reference 1, respectively. Veeder and Schankula's Eqs. (11) and (20) do not properly taken into account the effects of the coolant temperature and film heat transfer coefficient variations, and Veeder and Schankula's equations (11) and (16) can not be derivable.

A systematic method of the generation of the input values of the physics, thermal hydraulic, and element and material performance parameters associated with the bowing formula was established with various computer codes such as RFSP, WIMS-AECL, NUCIRC, COBRA and ELESTRES.

The two bundles in the CANDU-6 highest power channel, N-6 were selected as the representative bundles for the present bowing analyses. One bundle B-4, which is either the 37- or 43-element bundle, has been operated with the high power of around 700 kW at the P-4 position in the operation of 100 to 280 FPDs and with the low power of around 150 kW at the downstream position of P-12 in the operation of 280 FFDs to the discharge at 490 FPDs. The other bundle B-6, which is either the 37- or 43 bundle, has been operated with the continuous highest power of around 800 kW at the P-6 position in the fuel string in the operating period of 100 FPDs to the discharge at 280 FPs.

(2) The results of the sensitivity study on the parameters affecting the thermally induced bowing of CANDU-6 fuel element indicates that the variations of the element length , the sheath inner radius, coolant temperature, pellet/sheath mechanical interaction factor, the neutron flux depression factor , element linear power, pellet thermal expansion coefficient and the pellet/sheath heat transfer coefficient greatly effect on the element bowing than those of other parameters such as the sheath thickness , film heat transfer, sheath thermal expansion coefficient, the sheath and pellet thermal conductivities. It is also noted that with the increase of the sheath thickness only, the bowing of the element with an asymmetric heat will be slowly and linearly raised, and, however, the bowing of the symmetric heat generated elements will be slowly and linearly reduced.

(3) The thermally induced element bows of the bundles operated with the stepwise powers is smaller than that of the bundles operated with a continue high powers.

In the 37-element bundles, a maximum value of the thermally induced element bowing occurs in the outer element (E4) of the bundle in the continuous high power operation. In the 43-element bundles, that occurs in the inner element (E2) of the bundle also in the in the continuous high power operation. Both the maximum bows are in the direction of the pressure tube wall. The maximum bowing (< 0.22 mm) of the element in the 37-element bundle is larger than that (< 0.12 mm) in the 43-element bundle during the in-reactor service or refuelling. The maximum bowing of the outer element in the 37-element bundle is relatively small at the early burnup and then reached the maximum level at the end of life time in the reactor. However, the bowing of the inner and intermediate elements is smaller than those of the outer elements, and decreases with the increase of burnup. The bows of all the inner, intermediate and outer elements of the 43-element bundle operated with the continue high powers are relatively high at the early burnup and then reached the minimum level at the end of life time in the reactor.

(4) Considering the integrity of fuel element and bundle as a function of operation conditions such as bundle and channel powers, the element bowing behaviour of the CANFLEX 43-element bundle could be more safe than that of the 37-element bundle during the in-reactor service or refuelling. This is one of advantages for the CANFLEX 43-element bundle in comparison with the standard 37-element bundle.

NOTATION

a, b	=	inner and outer radii of sheath ($b = a + t$)
D	=	neutron flux gradient factor, defined in text
G	=	the mechanical interaction factor between 0 and 1.
h_{fs}	=	heat transfer coefficient between fuel and sheath
h_{sc}, $\bar{h}_{sc}$	=	local and average film heat transfer coefficients between sheath and coolant
Is	=	moment of inertia for sheath
K_1 to K_4	=	quantities defined in text.
l	=	unrestrained length of fuel element
q'	=	power per unit fuel length
r, θ	=	cylindrical coordinates of point P with respect to axis of element (see Fig. 2)
R_i, R	=	distances of element axis and point P from bundle axis (see Fig. 2)
t	=	sheath thickness ($t = b - a$)
$\bar{T}c$	=	average coolant temperature
$T(r,\theta)$	=	temperature at point P
$\bar{w}$	=	average heat flux of the element
α, α_s	=	thermal expansion coefficients of fuel and sheath
β, γ	=	quantities defined in text relating to variation of coolant temperatures and film heat transfer, respectively.
δ	=	magnitude of bow
ΔT_p	=	difference between maximum and minimum sheath surface temperatures
κ	=	inverse diffusion length for thermal neutrons in homogenized bundle (fuel, sheath and coolant)
λ, λ_s	=	thermal conductivity of fuel and sheath

REFERENCES

1. J. VEEDER and M.H. SCHANKULA, "Bowing of Pelletized Fuel Element - Theory and In-Reactor Experiments", Nuclear Engineering and Design 29(1974)167-179.
2. M. GACESA, V.C. ORPEN and OLDAKER, "CANDU Fuel Design: Current Concepts", Presented in IAEA/CENA International Seminar on Heavy Water Fuel Technology, San Carlos de Bariloche, 1983 June 27~July 1; AECL Report AECL-MISC 250-1(Rev.1), 1983 November.
3. M. Tayal, "Modelling the Bending/Bowing of Composite Beam such as Nuclear Fuel: The BOW Code", Nuclear Engineering and Design 116(1989)149-159.
4. H. C. Suk, K.S. Sim, J.H. Park, G.S. Park, T.S. Byun, C.J. Jeong "Re-Derivation and Assessment of Thermally-Induced Fuel Element Bowing for BOW Code", KAERI Report, KAERI-TR-493/94, February 1995.
5. A.D. LANE, H.C. SUK, et al.,"Recent Achievement in the Joint AECL/KAERI Program to Develop the CANFLEX Fuel Bundle", Presented at KAIF/KNS Annual Counference, Seoul, 1995 April 6~7.
6. B. A. Boley and J. H. Weiner, "Theory of Thermal Stress", John Wiley & Sons, Inc., New York (1960), page 310
7. M. Tayal, " Modelling CANDU Fuel under Normal Operating Conditions; ELESTRES Code Description", AECL report, AECL-9331, February 1987.
8. D. A. JENKINS and B. ROUBEN, "Reactor Fuelling Simulation Program - RFSP: User's Manual for Microcomputer Version", TTR-321, AECL-CANDU.
9. J. V. Donnelly, "WIM-AECL, a User's Manual for the Chalk River Version of WIMS", AECL report, AECL-8955, 1986.
10. B. CHEXAL, "NUCIRC: A Computer Code for Nuclear Heat Transport Circuit Thermohydraulic Analysis", AECL Internal Report TDAI, January 1977.
11. D. S. Rowe, "COBRA IIIC, a Digital Computer Program for Steady-State and Transient Thermal-Hydraulic of a Rod Bundle Nuclear Fuel Elements", BNWL-1695, Battelle, Richland, Washington, March 1973.
12. "MATPRO-version 09; A Handbook of Materials Properties for Use in the Analysis of Light Water Reactor Fuel Rod Behaviour", Edited by P. E. MacDonald, L. B. Thompson, TREE-NUREG-1005, EG & G Idaho, December 1976.

Table 1. Numerical Values * of CANDU-6 Fuel Element Parameters used for the Sensitivity Calculations

Parameter	Value	Parameter	Value	Parameter	Value
a (mm)	6.12	t (mm)	0.42	l (mm)	500
D (fraction)	0.030	q' (kW/m)	51.6	α_s (μm/m K)	4.4
α (μm/m K)	11.0	λ_s (kW/m K)	0.016	λ (kW/m K)	0.003
$\bar{h}$ (kW/m^{2}K)	50.0	γ (fraction)	0.026	h_{fs} (kW/m^{2}K)	9.86
$\bar{T}$ (°C)	300	β (fraction)	0.0048	G (fraction)	1.0

* The values are assumed for the present calculations to explain bowing in CANDU type fuel elements without having to invoke other mechanisms such as compressive axial loads.

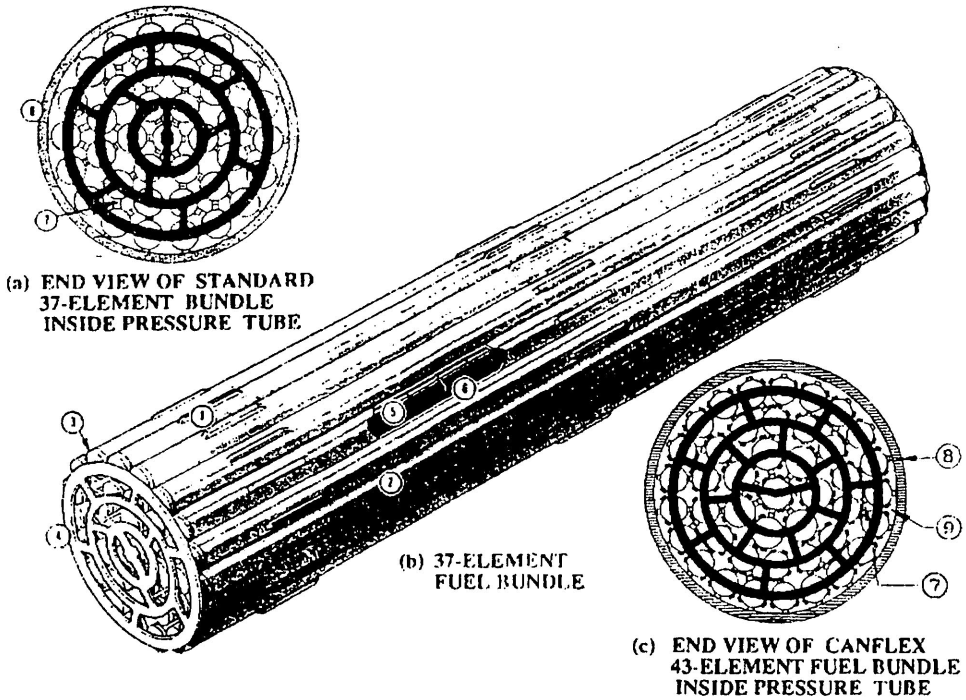

1. Zircaloy Bearing Pads	2. Zircaloy Fuel Sheath	3. Zircaloy End Cap
4. Zircaloy End Support Plate	5. Uranium Dioxide Pellets	6. Graphite Interlayer
7. Inter Element Spacers	8. Pressure Tube	9. CHF Enhancement Pads*

* The CHF enhancement pas are located in the two planes between the middle bearing pads and outer bearing pads of CANFLEX bundle.

FIG. 1. STANDARD 37-ELEMENT AND CANFLEX 43-ELEMENT FUEL BUNDLES

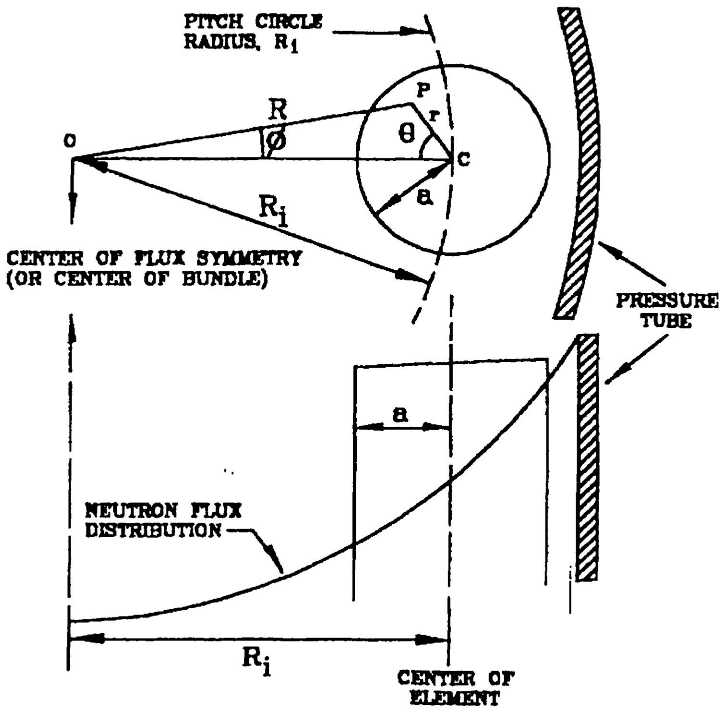

FIG. 2. COORDINATE SYSTEM USED IN THE ANALYSIS

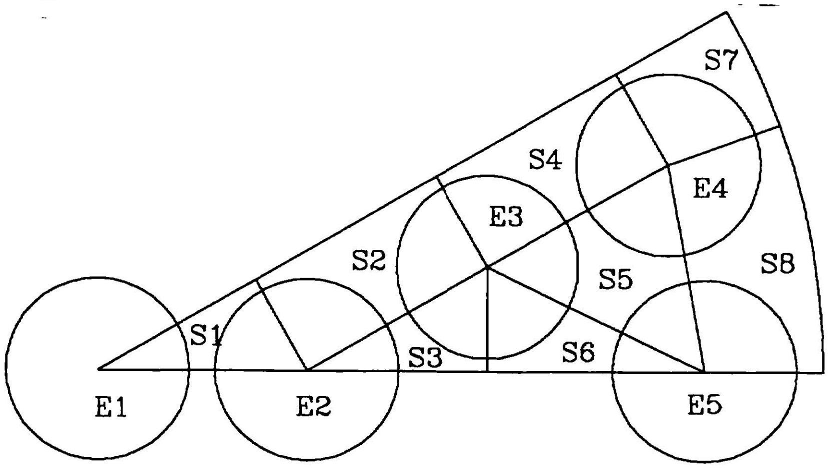

(A) 1/12 SYMMETRIC GEOMETRY OF 37-ELEMENT BUNDLE

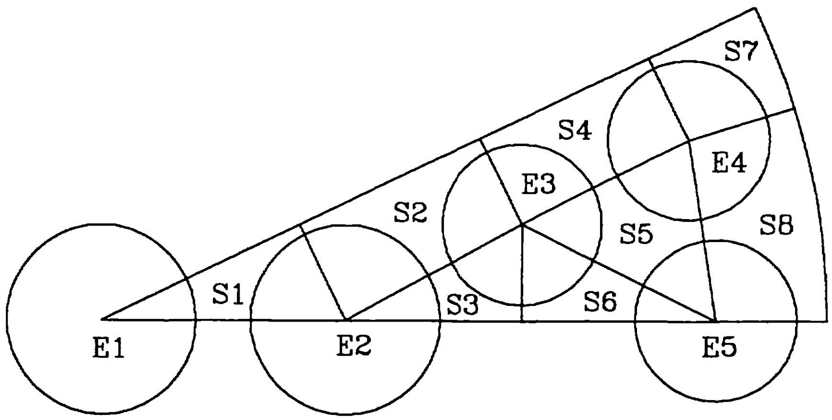

(B) 1/14 SYMMETRIC GEOMETRY OF 43-ELEMENT BUNDLE

FIG. 3. GEOMETRIES FOR THE SUBCHANNEL THERMALHYDRAULIC ANALYSIS OF THE 37- AND 43-ELEMENT BUNDLES

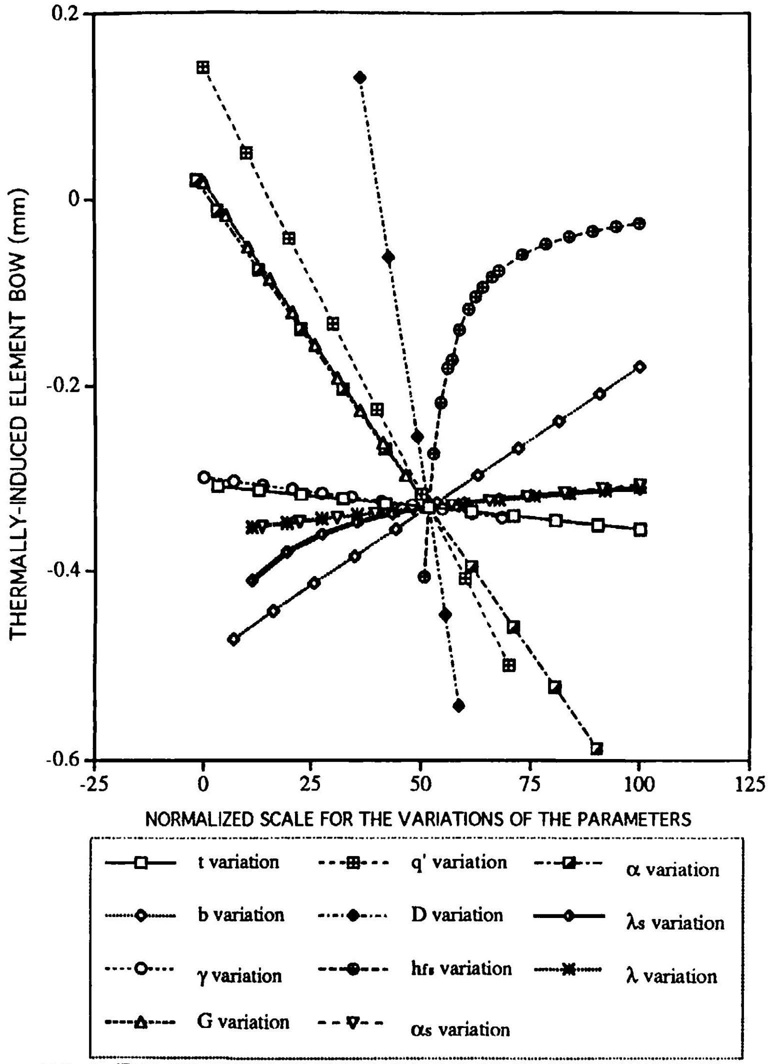

FIG. 4. THE SENSIVITY OF THE PARAMETERS ON THE BOWING OF ELEMENT WITH ASYMMETRIC HEAT, BASED ON TABLE 1

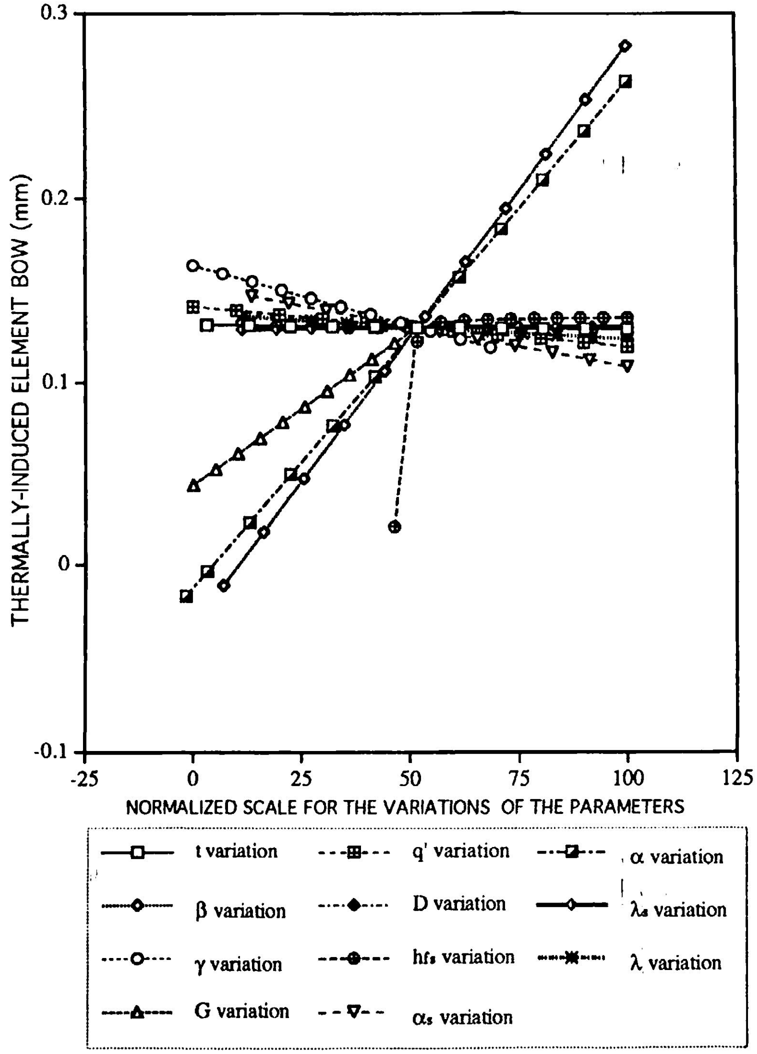

FIG. 5. THE SENSITIVITY OF THE PARAMETERS ON THE BOWING OF ELEMENT WITH SYMMETRIC HEAT, BASED ON TABLE 1

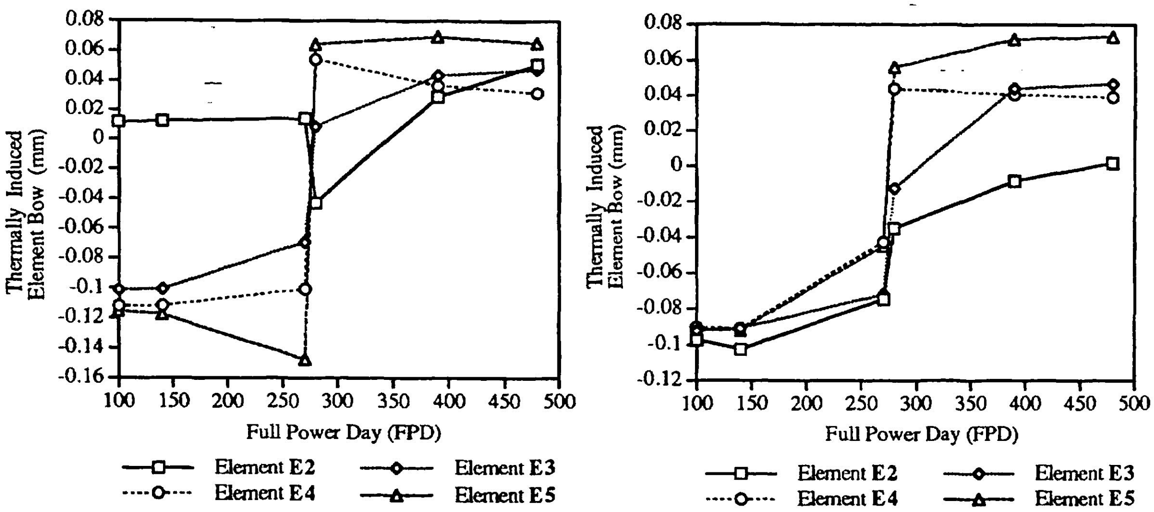

(A) Thermally Induced Element Bows of 37-Element Bundle B-4 (B) Thermally Induced Element Bows of 43-Element Bundle B-4

FIG. 6. THE THERMALLY INDUCED ELEMENT BOWS OF THE 37- AND 43-ELEMENT BUNDLES B-4 IN N-6 CHANNEL, PREDICTED AT 100, 140, 270, 280, 390 AND 480 FPD OF CANDU-6 REACTOR

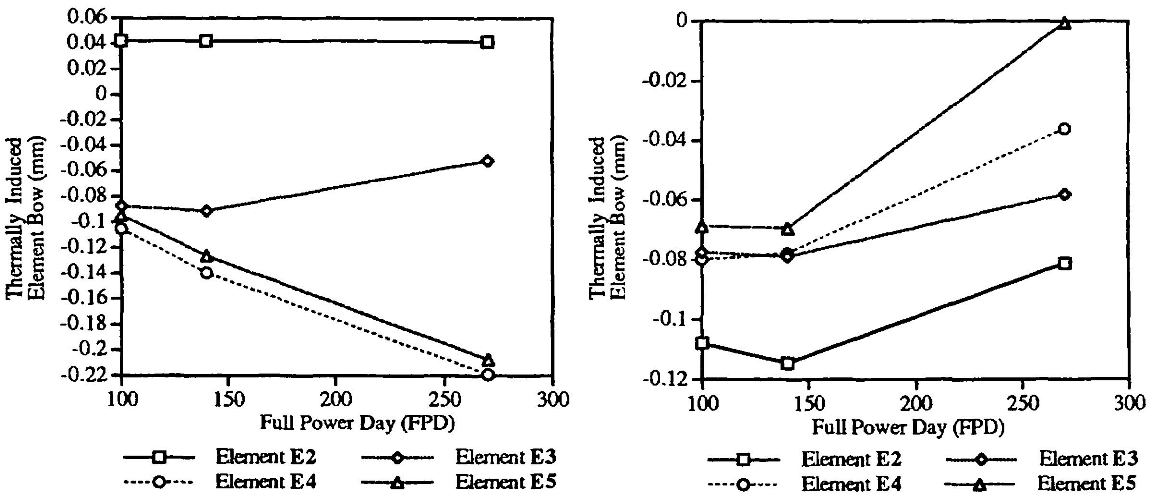

(A) Thermally Induced Element Bows of 37-Element Bundle B-6 (B) Thermally Induced Element Bows of 43-Element Bundle B-6

FIG.7. THE THERMALLY INDUCED ELEMENT BOWS OF THE 37- AND 43-ELEMENT BUNDLES B-6 IN N-6 CHANNEL, PREDICTED AT 100, 140 AND 270 FPD OF CANDU-6 REACTOR